








# Sheptide A: an antimalarial cyclic pentapeptide from a fungal strain in the *Herpotrichiellaceae*

Robert A. Shepherd<sup>1</sup> · Cody E. Earp<sup>1</sup> · Kristof B. Cank<sup>1</sup> · Huzefa A. Raja<sup>1</sup>  · Joanna Burdette<sup>2</sup>  · Steven P. Maher<sup>3</sup> · Adriana A. Marin<sup>3</sup> · Anthony A. Ruberto<sup>3</sup>  · Sarah Lee Mai<sup>3</sup> · Blaise A. Darveau<sup>4</sup> · Dennis E. Kyle<sup>3</sup> · Cedric J. Pearce<sup>4</sup>  · Nicholas H. Oberlies<sup>1</sup> 

Received: 14 December 2022 / Revised: 28 August 2023 / Accepted: 1 September 2023  
© The Author(s) 2023. This article is published with open access

## Abstract

As part of ongoing efforts to isolate biologically active fungal metabolites, a cyclic pentapeptide, sheptide A (**1**), was discovered from strain MSX53339 (*Herpotrichiellaceae*). The structure and sequence of **1** were determined primarily by analysis of 2D NMR and HRMS/MS data, while the absolute configuration was assigned using a modified version of Marfey's method. In an in vitro assay for antimalarial potency, **1** displayed a pEC<sub>50</sub> value of 5.75 ± 0.49 against malaria-causing *Plasmodium falciparum*. Compound **1** was also tested in a counter screen for general cytotoxicity against human hepatocellular carcinoma (HepG2), yielding a pCC<sub>50</sub> value of 5.01 ± 0.45 and indicating a selectivity factor of ~6. This makes **1** the third known cyclic pentapeptide biosynthesized by fungi with antimalarial activity.

## Introduction

Malaria continues to be one of mankind's most lethal diseases, causing an estimated 627,000 deaths and 241 million infections in 2020 alone [1, 2]. *Plasmodium falciparum*, one species of protozoan parasite causing malaria, is responsible for the most malaria infections in humans [3]. Unfortunately, *Plasmodium* species have shown resistance to core antimalarial drugs, including artemisinin and quinine, presenting a need for new antimalarial drug leads [4–6].

There are estimated to be millions of fungal species [7, 8], but fewer than 150,000 have been described taxonomically

[7], and it is likely that even a smaller portion of these have been studied for the production of bioactive secondary metabolites [9]. With the goal of discovering antimalarial drug leads from filamentous fungi, a cyclic pentapeptide, sheptide A (**1**), was discovered from fungal strain MSX53339, a member of the family *Herpotrichiellaceae*, and shown to be active against *P. falciparum*.

At least fifty-seven cyclic pentapeptides have been isolated from a variety of fungal genera, such as *Aspergillus*, *Clonostachys*, *Fusarium*, *Hamigera*, *Penicillium*, *Pseudallescheria*, and *Xylaria* [10, 11]. This class of compounds has exhibited a wide range of biological activities, including antibacterial (avellanin A), antifungal [cyclo(L-Phe- L-Leu- L-Leu- L-Leu- L-Leu)], antiviral (aspergillipeptide D), chitinase inhibition (argadin), cytotoxic (cycloaspeptide F), immunosuppressive (pseudacyclin A), insecticidal (cycloaspeptide E), and vasoconstriction (avellanin A) activities [10, 12–14]. Currently, cycloaspeptides A and D are the only other cyclic pentapeptides isolated from fungi that exhibit antimalarial activity [10, 12–15], and we add to this via the discovery of **1** (Fig. 1).

## Results and discussion

An extract of fungal strain MSX53339 was studied as part of a new collaboration, where we are examining a diverse

**Supplementary information** The online version contains supplementary material available at <https://doi.org/10.1038/s41429-023-00655-6>.

✉ Nicholas H. Oberlies  
n\_oberli@uncg.edu

<sup>1</sup> Department of Chemistry & Biochemistry, University of North Carolina at Greensboro, Greensboro, NC, USA

<sup>2</sup> Department of Pharmaceutical Sciences, University of Illinois Chicago, Chicago, IL, USA

<sup>3</sup> Center for Tropical & Emerging Global Diseases, University of Georgia, Athens, GA, USA

<sup>4</sup> Mycosynthetix, Inc., Hillsborough, NC, USA

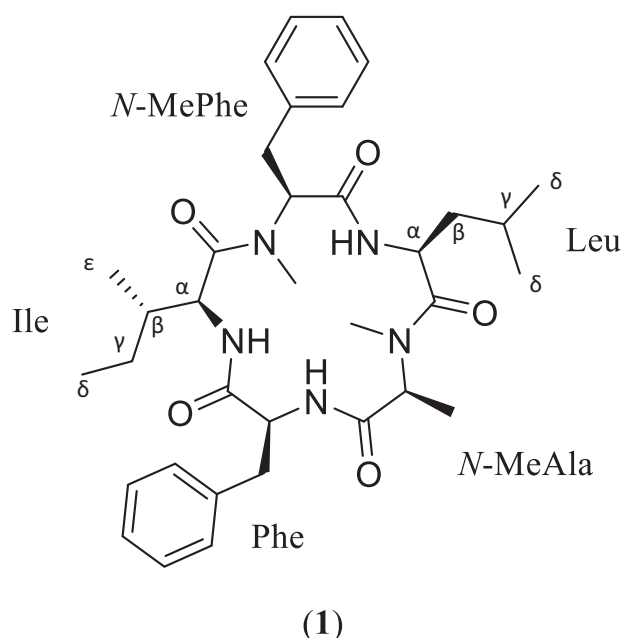


**Fig. 1** Structure and amino acid sequence of the cyclic pentapeptide, sheptide A (**1**)

library of fungal cultures for antimalarial activity. A key goal is to identify leads that are more toxic to the *P. falciparum* parasite than they are generally cytotoxic to human cells [16, 17]. In this case, the lack of general cytotoxicity of this fungal extract (i.e.  $IC_{50}$  values  $> 20 \mu g\ ml^{-1}$  vs a panel of cancer cell lines) [18], coupled with promising dereplication data [19, 20], led us to further investigate the chemical diversity [21, 22] of this fungus for antimalarial potential.

Sheptide A (**1**) was isolated as a clear solid, and its molecular formula was determined as  $C_{35}H_{49}N_5O_5$  by HRMS/MS, based on an  $m/z$  of 620.3787 (calcd for  $C_{35}H_{50}N_5O_5$ ,  $m/z$  620.3812) for  $[M + H]^+$ , indicating an index of hydrogen deficiency of 14. The molecular formula matched that of the cyclic pentapeptides, persipeptides A and B, which were isolated from a *Streptomyces* species [23]. While there were similarities in the  $^1H$  and  $^{13}C$  NMR spectra of **1** and those of the persipeptides, **1** differed by three amino acid residues. Specifically, valine and *N*-methylvaline residues in the persipeptides were replaced by leucine, isoleucine, and *N*-methylalanine in the structure of **1**.

The  $^1H$  and  $^{13}C$  spectra of **1** (DMSO- $d_6$ ; Table 1, Fig. S1) indicated the presence of seven methyls (including two *N*-methyls), three *N*-H protons, four methylenes, seven methines, two phenyls, and five carbonyls. Spectroscopy signatures for phenylalanine (Phe), *N*-methylalanine (*N*-MeAla), isoleucine (Ile), *N*-methylphenylalanine (*N*-MePhe), and leucine (Leu) were evident in the HSQC and  $H^1-H^1$  TOCSY data (Figs. S2, S4). These findings

accounted for 13 of the 14 degrees of unsaturation, with the final one resolved by the macrocycle.

The amino acid sequence was determined by extensive use of HMBC and NOESY correlations and further confirmed by HRMS/MS (Fig. S10). The presence of two phenyl and three aliphatic residues made deciphering the  $^1H$  spectrum of **1** (Fig. S1) more challenging due to peak overlap. A prime example was at 3.28 ppm, where one of the  $\beta$ -CH<sub>2</sub> proton signals was obscured by a residual water peak at 3.30 ppm, such that the correlation was only evident in the HSQC spectrum. The second case was at 7.14 ppm, where a third *N*-H proton signal was masked by the phenyl signals, as determined using COSY and TOCSY correlations. Additionally, some  $^1H$  NMR signals that resembled complex multiplets were determined to be two overlapping signals, including the  $\alpha$ -CH signals of Phe and Leu at 4.72 ppm and 4.76 ppm, respectively, the aliphatic  $\beta$ -CH<sub>2</sub> signals of Phe and *N*-MePhe at 2.76 ppm and 2.80 ppm, respectively, and the  $\delta$ -CH<sub>3</sub> proton signals for Leu at 0.84 and 0.86 ppm. Based on HRMS/MS data, the initial sequence was determined to be *N*-MePhe<sup>1</sup>-Ile/Leu<sup>2</sup>-*N*-MeAla<sup>3</sup>-Phe<sup>4</sup>-Ile/Leu<sup>5</sup> (Fig. S10). COSY and TOCSY correlations were used to confirm the spin systems of the individual amino acid residues (Fig. 2). Then, key HMBC and NOESY correlations were used to confirm their relative positions in the sequence.

Analysis of COSY and TOCSY spectra of **1** (Figs. S3, S4) was helpful in distinguishing the Ile and Leu residues, which can be challenging to differentiate, as they have the same monoisotopic mass and similar 1D NMR chemical shifts. The discerning feature between these residues is the presence of two nearly identical  $\delta$ -methyl groups on Leu ( $\delta_H$  0.84 and 0.86 ppm), which resonate as two overlapping doublets in the  $^1H$  NMR spectrum (Fig. S1) that are both coupled to the  $\gamma$ -CH proton of Leu ( $\delta_H$  1.49 ppm) as determined by COSY and confirmed by a  $J$  value of 6.6 Hz. These methyl groups also show  $^1H$ - $^1H$  TOCSY correlations with the  $\beta$ -methylene protons and the  $\alpha$ -proton ( $\delta_H$  1.23, 1.79, and 4.76 ppm respectively). In contrast, Ile has one terminal methyl and one secondary methyl, both of which show diagnostic chemical shifts and splitting patterns in the  $^1H$  NMR spectrum (Fig. S1). The terminal methyl ( $\delta_H$  0.52 ppm) had an indistinct splitting pattern, likely due to coupling with the two diastereotopic protons on the  $\gamma$ -methylene of Ile ( $\delta_H$  0.49 and 0.78 ppm). The secondary  $\epsilon$ -methyl ( $\delta_H$  0.13 ppm) displayed as a doublet due to coupling with the adjacent  $\beta$ -methine proton ( $\delta_H$  1.34 ppm), which was also determined by COSY. Additionally, both methyls displayed  $^1H$ - $^1H$  TOCSY correlations with the other protons in the Ile spin system. In summary, distinguishing between Ile and Leu was possible after considering the data from multiple NMR experiments.

To confirm the amino acid sequence of **1**, key HMBC and NOESY correlations between respective residues were

**Table 1** NMR data for **1** [700 MHz ( $^1\text{H}$ ) and 175 MHz ( $^{13}\text{C}$ ) in  $\text{DMSO}-d_6$ ]

Amino Acid	Position	$^{13}\text{C}$	$^1\text{H}$ (mult., $J$ in Hz)	HMBC	NOESY
Phe	C = O	169.9	—	—	—
	NH	—	7.14 (buried)	55.7, 168.8	2.32, 2.70, 2.80, 2.97, 3.28, 4.07, 4.17, 4.72
	$\alpha$ -CH	55.7	4.72 (m)	38.2, 169.9	7.91
	$\beta$ -CH <sub>2</sub>	38.2	2.76 (dt, 14.3, 10.6)	55.7, 129.4, 136.9, 169.9	—
			2.97 (dd, 14.3, 6.9)	55.7, 129.4, 136.9, 169.9	—
	$\gamma$ -C (ar.)	136.9	—	—	—
	$\delta$ -CH(1) (ar.)	129.4*	7.14*	38.2, 127.2*	2.32, 2.70, 2.80, 2.97, 3.28, 4.07, 4.17, 4.72
	$\delta$ -CH(2) (ar.)	129.0*	7.14*	38.2, 127.2*	2.32, 2.70, 2.80, 2.97, 3.28, 4.07, 4.17, 4.72
	2x $\epsilon$ -CH (ar.)	128.8	7.25	128.8*, 129.0*, 129.4*, 136.9	0.13, 3.36
N-Me Ala	$\zeta$ -CH (ar.)	127.2	7.18	—	2.32
	C = O	168.8	—	—	—
	N-CH <sub>3</sub>	29.7	2.32 (s)	55.9, 169.8	0.52, 0.86*, 1.17, 2.70, 4.17, 4.76, 7.14
	$\alpha$ -CH	55.9	4.17 (1, 6.9)	15.2, 29.7, 168.8	2.32, 4.76, 7.14
Ile	$\beta$ -CH <sub>3</sub>	15.2	1.17 (d, 6.9)	55.9, 168.8	1.34, 2.32, 2.70
	C = O	170.8	—	—	—
	NH	—	7.91 (d, 8.7)	52.8, 169.9	0.13, 1.34, 2.32, 2.80, 2.97, 4.07, 4.72, 7.14, 7.34
	$\alpha$ -CH	52.8	3.36 (dd, 8.7, 8.2)	24.1, 36.7, 170.8	0.13, 0.52, 0.78, 4.07, 7.14
	$\beta$ -CH <sub>2</sub>	36.7	1.34 (m)	12.1, 24.1, 52.8	3.36, 7.91
	$\epsilon$ -CH <sub>3</sub>	15.4	0.13 (d, 6.7)	24.1, 36.7, 52.8	0.52, 2.70
	$\gamma$ -CH <sub>2</sub>	24.1	0.49 (m)	—	0.78, 3.36
			0.78 (dd, 18.8, 6.7)	—	—
	$\delta$ -CH <sub>3</sub>	12.1	0.52 (m)	24.1, 36.7	0.86*, 3.36
N-Me Phe	C = O	168.4	—	—	—
	N-CH <sub>3</sub>	31.3	2.70 (s)	61.7, 170.8	0.13, 0.52, 0.86*, 1.17, 2.30, 3.36, 4.07, 7.14, 7.34
	$\alpha$ -CH	61.7	4.07 (m)	31.3, 34.7, 137.8, 168.4	2.70, 3.36, 7.14, 7.34, 7.91
	$\beta$ -CH <sub>2</sub>	34.7	2.80 (dt, 14.3, 10.6)	129.4	7.14, 7.91
			3.28 (buried)	61.7, 129.4, 137.8	7.14
	$\gamma$ -C (ar.)	137.8	—	—	—
	$\delta$ -CH(1) (ar.)	129.4*	7.14*	34.7, 127.2*	2.32, 2.70, 2.80, 2.97, 3.28, 4.07, 4.17, 4.72
	$\delta$ -CH(2) (ar.)	130.2*	7.14*	34.7, 127.2*	2.32, 2.70, 2.80, 2.97, 3.28, 4.07, 4.17, 4.72
	2x $\epsilon$ -CH (ar.)	128.8	7.25	128.8*, 129.0*, 129.4*, 137.8	0.13, 3.36
Leu	$\zeta$ -CH (ar.)	127.2	7.18	—	2.32
	C = O	169.8	—	—	—
	NH	—	7.34 (d, 9.4)	47.6, 168.4	2.32, 2.70, 4.07, 4.17
	$\alpha$ -CH	47.6	4.76 (d, 9.4)	169.8	0.86*, 1.49, 2.32, 4.17
	$\beta$ -CH <sub>2</sub>	42.4	1.23 (dt, 13.3, 6.6)	22.9, 47.6, 169.8	0.84*, 0.86*, 1.49, 2.70
			1.79 (dt, 13.3, 7.1)	—	0.84*, 0.86*
	$\gamma$ -CH	24.8	1.49 (dq, 13.3, 6.6)	22.9, 42.4, 47.6	4.76
	$\delta_1$ -CH <sub>3</sub>	22.9	0.84 (d, 6.6)	22.9, 24.8, 42.4	0.52, 1.23, 1.79, 2.32, 2.70, 4.76
	$\delta_2$ -CH <sub>3</sub>	23.2	0.86 (d, 6.6)	22.9, 24.8, 42.4	0.52, 1.23, 1.79, 2.32, 2.70, 4.76

\*Values can be interchangeable

examined. Based on the HRMS/MS data, NMR confirmation of the peptide sequence started with the *N*-MePhe residue. An HMBC correlation between the NH proton of Leu ( $\delta_{\text{H}}$  7.34) and the carbonyl carbon of *N*-MePhe ( $\delta_{\text{C}}$  168.4) indicated that Leu was acylated by *N*-MePhe. This was supported by NOESY correlations between the NH proton of Leu ( $\delta_{\text{H}}$  7.34) and the *N*-CH<sub>3</sub> protons of *N*-MePhe

( $\delta_{\text{H}}$  2.70). An HMBC correlation between the *N*-CH<sub>3</sub> protons of *N*-MeAla ( $\delta_{\text{H}}$  2.32) and the carbonyl carbon of Leu ( $\delta_{\text{C}}$  168.4) was observed, indicating acylation of *N*-MeAla by Leu. This was confirmed by NOESY correlations between both the  $\alpha$ -protons of *N*-MeAla and Leu ( $\delta_{\text{H}}$  4.17 and  $\delta_{\text{H}}$  4.76 respectively) and between the NH proton of Leu ( $\delta_{\text{H}}$  7.34) and the *N*-CH<sub>3</sub> protons of *N*-MeAla ( $\delta_{\text{H}}$  2.32).

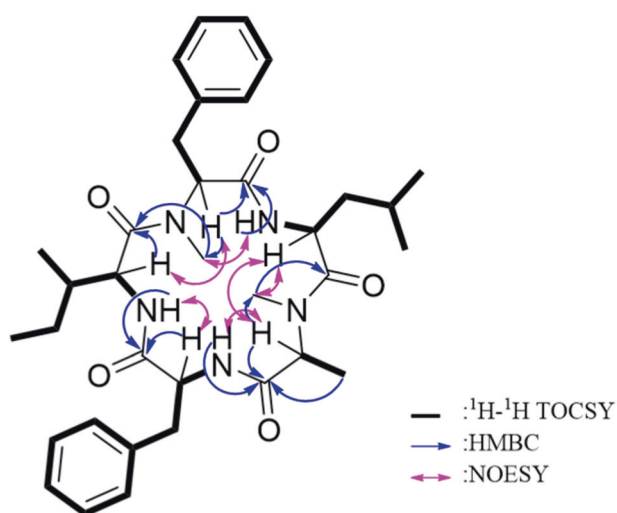


**Fig. 2** Key 2D NMR correlations for sheptide A (**1**)

This partial sequence fragment of *N*-MePhe<sup>1</sup>-Leu<sup>2</sup>-*N*-MePhe<sup>3</sup> was confirmed by the HRMS/MS spectrum (i.e., *m/z* 360.2020). Next, an HMBC correlation between the *N*-H proton on Phe ( $\delta_{\text{H}}$  7.14) and the carbonyl carbon on *N*-MeAla ( $\delta_{\text{C}}$  168.8) indicated acylation of Phe by *N*-MeAla. NOESY correlations between the  $\alpha$ -protons of Phe and *N*-MeAla ( $\delta_{\text{H}}$  4.72 and  $\delta_{\text{H}}$  4.17 respectively) and between the *N*-H proton of Phe and the *N*-CH<sub>3</sub> protons of *N*-MeAla confirmed this connection. This was supported by a fragment in the HRMS/MS spectrum (i.e., *m/z* 507.2636), which was indicative of the aforementioned fragment plus the mass of Phe. This left the positioning of the Ile residue, which was placed between the Phe and *N*-MePhe residues, as confirmed by HMBC correlations between the *N*-H proton of Ile ( $\delta_{\text{H}}$  7.91) and the carbonyl carbon of Phe ( $\delta_{\text{C}}$  169.9), as well as, between the *N*-CH<sub>3</sub> protons of *N*-MePhe ( $\delta_{\text{H}}$  2.70) and the carbonyl carbon of Ile ( $\delta_{\text{C}}$  170.8). This finding was buttressed by NOESY correlations between both the *N*-H protons of Ile and Phe ( $\delta_{\text{H}}$  7.91 and  $\delta_{\text{H}}$  7.14 respectively) and between the  $\alpha$ -protons of *N*-MePhe and Ile. Thus, the final cyclic peptide sequence was *N*-MePhe<sup>1</sup>-Leu<sup>2</sup>-*N*-MeAla<sup>3</sup>-Phe<sup>4</sup>-Ile<sup>5</sup> (Fig. 1).

The absolute configuration of the amino acids was determined using a modified Marfey's method [24]. After subjecting **1** to acid hydrolysis followed by derivatization with Marfey's reagent, the 1-fluoro-2,4-dinitrophenyl-5-L-alanine amide derivatives of each amino acid in **1** were subjected to LC-MS analysis along with derivatized standards of both D and L amino acids. Comparison of retention times and mass data revealed that the amino acid residues all had the L-configuration (Fig. S8).

Compound **1** was next evaluated as a potential drug lead for antimalarial activity, where it would be desirable to both kill the parasite but not be generally cytotoxic to eukaryotic cells. Against the parasite, *P. falciparum*, it displayed a

$\text{pEC}_{50}$  value of  $5.75 \pm 0.49$ . Alternatively, when tested in a standard counter screen for general toxicity against human hepatocellular carcinoma (HepG2) [25], moderate cytotoxicity was observed ( $\text{pCC}_{50}$  value of  $5.01 \pm 0.49$ ). In examining the difference in anti-plasmodial vs cytotoxic activities, compound **1** exhibited approximately 6-fold selectivity for the parasite (Fig. S13). As a starting point for uncovering antimalarial leads, this level of selectivity is consistent with other fungal metabolites [26–29].

## Conclusions

A new cyclic pentapeptide, sheptide A (**1**), was isolated from a fungus of the family *Herpotrichiellaceae* (strain MSX53339) and was composed of the amino acid sequence *N*-MePhe<sup>1</sup>-Leu<sup>2</sup>-*N*-MeAla<sup>3</sup>-Phe<sup>4</sup>-Ile<sup>5</sup>. A suite of 2D NMR and HRMS/MS experiments were used to establish this sequence, and a modified Marfey's method was used to determine the absolute configuration of the amino acid building blocks, which were all L. Compound **1** had approximately 6-fold selectivity for *P. falciparum* and represents the third reported cyclic pentapeptide of fungal origin with anti-plasmodial activity. Further studies are ongoing to modify the structure of **1**, with a goal of enhancing anti-plasmodial activity, minimizing cytotoxicity to eukaryotic cells, and developing a molecule that could be patented [30].

## Materials and methods

### General experimental procedures

Optical rotation, UV, and IR data were obtained using a Rudolph Research Autopol III polarimeter (Rudolph Research Analytical), an Agilent Cary Series UV-vis Spectrophotometer (Agilent Technologies), and a PerkinElmer Spectrum 65 FT-IR Spectrometer with Universal ATR attachment (PerkinElmer). NMR data were obtained using either a JEOL ECA-500 MHz NMR spectrometer operating at 500 MHz for <sup>1</sup>H and 125 MHz for <sup>13</sup>C (JEOL Ltd.) or an Agilent 700 MHz NMR spectrometer (Agilent Technologies, Inc.) equipped with a cryoprobe, operating at 700 MHz for <sup>1</sup>H and 175 MHz for <sup>13</sup>C. Residual solvent signals of DMSO ( $\delta_{\text{H}}$  = 2.50 and  $\delta_{\text{C}}$  = 39.5) were used as reference peaks. HRMS/MS data were collected via either a Thermo Fisher Scientific LTQ Orbitrap XL mass spectrometer or a Thermo Fisher Scientific Q Exactive Plus mass spectrometer, both equipped with a heated electrospray ionization (HESI) source (Thermo Fisher Scientific) and connected to a Waters Acquity UPLC system. A Phenomenex Kinetix C<sub>18</sub> column (1.3  $\mu\text{m}$ ; 50  $\times$  2.1 mm), heated to 40 °C, was operated at a flow rate of 0.3 ml min<sup>−1</sup> with a gradient system of 15:85 to 100:0 of CH<sub>3</sub>CN-H<sub>2</sub>O

(0.1% formic acid) over 10 min. MS data were collected from  $m/z$  150 to 2000 in the positive mode. A Varian Prostar HPLC system, equipped with ProStar 210 pumps and a Prostar 335 photodiode array detector (PDA), was used to conduct all analytical and preparative HPLC experiments, with data collected and analyzed using Galaxie Chromatography Workstation software (version 1.9.3.2, Varian Inc.). All chromatography were conducted on Gemini-NX  $C_{18}$  analytical (5  $\mu$ m; 250  $\times$  4.6 mm), semipreparative (5  $\mu$ m; 250  $\times$  10 mm), or preparative (5  $\mu$ m; 50  $\times$  21.2 mm) columns (all from Phenomenex). Flash chromatography was performed on a Teledyne ISCO CombiFlash Rf 200 using Silica Gold columns (from Teledyne Isco) and monitored by UV and evaporative light-scattering detectors.

### Fungal strain identification and fermentation

Fungal strain MSX53339 was isolated in 1991 from leaf litter that was collected in a baboon sanctuary. Examination of cultural morphology grown on malt extract agar did not reveal any sporulating structures, making identification of this strain based on morphology ambiguous. Molecular sequences from the internal transcribed spacer region, ITS rDNA (specifically ITS1, 5.8 S, and ITS2), were obtained using primers ITS1F and ITS4 [31, 32]. Detailed methods for PCR and Sanger sequencing protocols were outlined previously [33]. A BLAST search in the NCBI database using the ITS region from the type and reference material [34] indicated relation to members of the family *Herpotrichiellaceae* Munk, in the order *Chaetothyriales*, Ascomycota. However, strain MSX53339 showed only  $\geq 80\%$  sequence homology with genera like *Capronia*, *Minimelanolocus*, and *Veronaea*. To further determine the phylogenetic disposition of this strain, we taxon sampled 10 of the 16 genera currently in the *Herpotrichiellaceae* [35]. Approximately 36 ITS sequences of *Herpotrichiellaceae* were obtained from a recent phylogenetic study [36] along with two outgroup taxa in the *Cyphellophoraceae*. Maximum likelihood analysis was implemented using IQ-TREE in PhyloSuite [37]. ModelFinder [38] was used to select the best-fit model using Akaike Information Criterion (AIC), and SYM + I + G4 was the best fit. Ultrafast bootstrapping was run with 5000 replicates [39]. Nodes with UFBoot  $\geq 90\%$  are shown on the clades, but only nodes  $\geq 95\%$  were considered strongly supported. Thus, strain MSX53339 was identified as a *Herpotrichiellaceae* sp. in the *Chaetothyriales*, Ascomycota (Figure S12). This strain is putatively a new genus or species within the *Herpotrichiellaceae*, but this hypothesis awaits further work due to the lack of morphological characters [40]. The sequence data were deposited in GenBank (ITS: OP207954 and OP207955).

The culture was stored on a malt extract slant and was transferred periodically. A fresh culture was grown on a

similar slant, and a piece was transferred to a medium containing 2% soy peptone, 2% dextrose, and 1% yeast extract (YESD media). Following incubation (7 d) at 22 °C with agitation, the culture was used to inoculate 50 ml of a rice medium, prepared using rice to which was added a vitamin solution and twice the volume of rice with  $H_2O$  in a 250-ml Erlenmeyer flask.

### Extraction and isolation

The solid-state fermentation culture was chopped into small pieces using a spatula, followed by the addition of 60 ml of 1:1 MeOH- $CHCl_3$  and was then shaken overnight ( $\sim 16$  h) at  $\sim 125$  rpm at rt. The resulting slurry was filtered in vacuo to form a filtrate, and the solid residue was rinsed with a small volume of 1:1 MeOH- $CHCl_3$ . To the filtrate, 90 ml of  $CHCl_3$  and 150 ml of  $H_2O$  were added; the solution was stirred for 20 min before being transferred to a separatory funnel. The organic layer was collected and evaporated to dryness under vacuum using a rotary evaporator. The resulting organic extract was then partitioned between 100 ml of 1:1 MeOH- $CH_3CN$  and 100 ml of hexanes. The MeOH- $CH_3CN$  layer was collected and evaporated to dryness under vacuum. The defatted organic extract ( $\sim 406$  mg) was reconstituted in  $CHCl_3$  and absorbed onto Celite 545. The extract was then fractionated using flash chromatography with a solvent gradient of hexane- $CHCl_3$ -MeOH at a 30 ml  $min^{-1}$  flow rate and 61.0 column volumes to yield four fractions. Fraction 3 ( $\sim 185$  mg) was further separated into 11 subfractions using preparative HPLC with a solvent gradient increasing linearly from 40:60 to 55:45  $CH_3CN$ - $H_2O$  (acidified with 0.1% formic acid) over 6 min, followed by an isocratic hold at 55:45  $CH_3CN$ - $H_2O$  (acidified with 0.1% formic acid) for five minutes, and finishing with another linear increase from 55:45 to 100:0  $CH_3CN$ - $H_2O$  (acidified with 0.1% formic acid) over nine minutes, all at a flow rate of 21.20 ml  $min^{-1}$ . Subfraction 9 yielded compound **1** (34.05 mg), which eluted at 21.5 min.

### Sheptide A (1)

Compound **1** was isolated as a clear solid (34.05 mg);  $[\alpha]_D^{20} = -80$  (c 0.001, MeOH) UV (MeOH)  $\lambda_{max}$  (log  $\epsilon$ ) 204 (4.56) nm; IR (diamond)  $\nu_{max}$  3299, 2957, 1630, 1530  $cm^{-1}$ ;  $^1H$  NMR (DMSO- $d_6$ , 500 MHz) and  $^{13}C$  NMR (DMSO, 125 MHz), Table 1 and Fig. S1; HR-HESI-MS  $m/z$  620.3787  $[M + H]^+$  (calcd for  $C_{35}H_{50}N_5O_5$ ,  $m/z$  620.3812).

### Modified Marfey's analysis

Approximately 0.2 mg of each amino acid standard was weighed into separate glass 2-ml reaction vials. To each



standard was added 50 ml of H<sub>2</sub>O, 20 ml of 1 M NaHCO<sub>3</sub>, and 100 ml 1% Marfey's reagent (*N*- $\alpha$ -(2,4-dinitro-5-fluorophenyl)-L-alaninamide) in acetone. The reaction mixtures were agitated at 40 °C for 1 h. The reactions were halted by the addition of 10 ml of 2 N HCl. The product of the reactions was dried under a stream of air and dissolved in ~1.7 ml of MeOH. Each derivatized standard was injected individually (0.7 ml) onto the UPLC. Also, aliquots of all the derivatized standards were combined to give a mixed standard, which was injected just prior to the digested and derivatized peptide **1**. UPLC conditions were 10–70% MeOH in H<sub>2</sub>O over 10 min on a BEH column and eluent monitored at 340 nm.

To generate the digested and derivatized peptide, approximately 0.2–0.3 mg of compound **1** was weighed into a 2-ml reaction vial, to which was added 0.5 ml of 6 N HCl. The compound was hydrolyzed at 110 °C for 24 h, at which time it was evaporated under a stream of air. To the hydrolysis product, 25 ml H<sub>2</sub>O, 10 ml 1 M NaHCO<sub>3</sub>, and 50 ml of 1% Marfey's reagent in acetone were added. The reaction mixture was agitated at 40 °C for 1 h. The reaction was halted by the addition of 5 ml of 2 N HCl. The mixtures were dried under a stream of air and brought up in ~200  $\mu$ l of MeOH and injected onto the UPLC with the use of the same conditions as for the standards.

### Cytotoxicity assay

Human melanoma cancer cells MDA-MB435 and human ovarian cancer cells OVCAR3 were purchased from the American Type Culture Collection. These cell lines were propagated at 37 °C in 5% CO<sub>2</sub> in RPMI 1640 medium, supplemented with fetal bovine serum (10%), penicillin (100 units/ml), and streptomycin (100  $\mu$ g ml<sup>-1</sup>). Cells in log phase growth were harvested by trypsinization followed by two washes to remove all traces of enzyme. A total of 5000 cells were seeded per well of a 96-well clear, flat-bottom plate (Microtest 96, Falcon) and incubated overnight (37 °C in 5% CO<sub>2</sub>). Samples dissolved in DMSO were then diluted and added to the appropriate wells. Taxol (paclitaxel) was used as a positive control.

### Antimalarial assay

A small aliquot of **1** was diluted to 10 mM in dehydrated, sterile DMSO (Tocris) and a duplicate-well, 12-point, 3-fold semilog dilution series was prepared at 1000 $\times$  final concentration in 384-well plates (Greiner Bio-one) in DMSO using a Biomek 4000 (Beckman Coulter). DMSO was plated as the negative control and dihydroartemisin was diluted from 1  $\mu$ M as the positive control. Source plates were sealed using foil sealing tape (VWR) and kept in a desiccator until used to inoculate *Plasmodium*

*falciparum* assay plates. Compounds were assayed using methods previously described [25]. Briefly, *P. falciparum* clone W2 [41, 42] was cultured in RPMI (Gibco) supplemented with 10% inactivated human plasma (Interstate Blood Bank) and 5% hematocrit (Interstate Blood Bank) as previously described [43]. Assays were started by adding 40  $\mu$ l of parasites at 2% parasitemia and 0.75% hematocrit to each well of 384-well plates (Greiner Bio-one) and then treated with **1** from the source plate using a 40 nl pin tool, resulting in a 1 $\times$  test concentration. After incubation for 72 h, plates were fixed with 0.1% glutaraldehyde (Electron Microscopy Resources) and stained with Hoechst 33342 (Thermo Fisher Scientific) overnight before high content imaging (HCI) with a 4 $\times$  objective on an ImageXpress Micro Confocal (Molecular Devices). Parasite DNA was quantified using built-in analysis software and normalized to positive and negative controls using CDD Vault. Compound **1** was tested in 5 independent experiments, and potency values listed represent the mean pEC<sub>50</sub> (calculated as the -log EC<sub>50</sub> [M]) from all replicates. To further investigate cytotoxicity, the same source plate containing a dilution series of compound **1** at 1000 $\times$  was used to treat HepG2 cells (ATCC HC-8065) seeded at 2000 cells/well in the same type of 384-well assay plate (Greiner) for 72 h. At the endpoint, plates were fixed with 4% paraformaldehyde (Thermo Fisher Scientific) and stained with Hoechst 33342, so that cell nuclei counts could be assessed by HCI, as above. Compound **1** was tested in 4 independent cytotoxicity experiments and potency values listed represent the mean pCC<sub>50</sub> (calculated as the -log EC<sub>50</sub> [M]) from all replicates.

### Data availability

The NMR data for **1** were deposited in the NP-MRD (<https://np-mrd.org/>) under accession number NP0331808.

**Acknowledgements** We dedicate this manuscript to the late Alan B. Shepard, Jr. who on May 5, 1961 became the first American in space. This research was supported by the National Institutes of Health via the National Institute of Allergy and Infectious Diseases through grant R21 AI163960 and via the National Cancer Institute through grant P01 CA125066. HCI data from drug studies were produced in the Biomedical Microscopy Core at the University of Georgia, which is supported by the Georgia Research Alliance. Some of the NMR studies were performed at the Joint School of Nanoscience and Nanoengineering, a member of the National Nanotechnology Coordinated Infrastructure (NNCI), which is supported by the National Science Foundation (Grant ECCS-2025462).

### Compliance with ethical standards

**Conflict of interest** The authors declare the following competing financial interest(s): NHO, CJP and HAR are members of the Scientific Advisory Board of Clue Genetics, Inc. NHO is also a member of the

Scientific Advisory Boards of Mycosynthetix, Inc and Ionic Pharmaceuticals, LLC.

**Publisher's note** Springer Nature remains neutral with regard to jurisdictional claims in published maps and institutional affiliations.

**Open Access** This article is licensed under a Creative Commons Attribution 4.0 International License, which permits use, sharing, adaptation, distribution and reproduction in any medium or format, as long as you give appropriate credit to the original author(s) and the source, provide a link to the Creative Commons licence, and indicate if changes were made. The images or other third party material in this article are included in the article's Creative Commons licence, unless indicated otherwise in a credit line to the material. If material is not included in the article's Creative Commons licence and your intended use is not permitted by statutory regulation or exceeds the permitted use, you will need to obtain permission directly from the copyright holder. To view a copy of this licence, visit <http://creativecommons.org/licenses/by/4.0/>.

## References

- World malaria report 2020: 20 years of global progress and challenges. World Health Organization: Geneva, 2020.
- World malaria report 2021. World Health Organization: Geneva, 2021.
- Bousema T, Drakeley C. Epidemiology and infectivity of *Plasmodium falciparum* and *Plasmodium vivax* gametocytes in relation to malaria control and elimination. *Clin Microbiol Rev*. 2011;24:377–410.
- Aminake MN, Pradel G. Antimalarial drugs resistance in *Plasmodium falciparum* and the current strategies to overcome them. *Microb Pathog Strateg Combating Them Sci Technol Educ*. 2013;1:269–82.
- Ashley EA, et al. Spread of artemisinin resistance in *Plasmodium falciparum* malaria. *N Engl J Med*. 2014;371:411.
- Singh V, et al. Designing and development of phthalimides as potent anti-tubulin hybrid molecules against malaria. *Eur J Med Chem*. 2022;239:114534.
- Lofgren LA, Stajich JE. Fungal biodiversity and conservation mycology in light of new technology, big data, and changing attitudes. *Curr Biol*. 2021;31:R1312–25.
- Lücking R, et al. Unambiguous identification of fungi: where do we stand and how accurate and precise is fungal DNA barcoding? *IMA Fungus*. 2020;11:14.
- Bills GF, Gloer JB. Biologically active secondary metabolites from the fungi. *Microbiol Spectr*. 2016;4:1–32.
- Wang X, Lin M, Xu D, Lai D, Zhou L. Structural diversity and biological activities of fungal cyclic peptides, excluding cyclodipeptides. *Molecules*. 2017;22:2069/2061.
- Dictionary of Natural Products. Taylor & Francis Group: London, 2021.
- Kim KW, et al. Structure of malformin B, phytotoxic metabolites produced by *Aspergillus niger*. *Tetrahedron Lett*. 1991;32:6715.
- Lewer P, et al. Discovery, synthesis, and insecticidal activity of cycloaspeptide E. *J Nat Prod*. 2006;69:1506–10.
- Zhang Y, Liu S, Liu H, Liu X, Che Y. Cycloaspeptides F and G, cyclic pentapeptides from a *Cordyceps*-colonizing isolate of *Isaria farinosa*. *J Nat Prod*. 2009;72:1364–7.
- Dalsgaard PW, Larsen TO, Christophersen C. Bioactive cyclic peptides from the psychrotolerant fungus *Penicillium algidum*. *J Antibiot*. 2005;58:141–4.
- Wells TNC. Natural products as starting points for future anti-malarial therapies: going back to our roots? *Malar J*. 2011;10:S3.
- Wells TNC, van Huijsduijnen RH, Van, Voorhis WC. Malaria medicines: a glass half full? *Nat Rev Drug Discov*. 2015;14:424–42.
- Aldrich LN, et al. Discovery of anticancer agents of diverse natural origin. *J Nat Prod*. 2022;85:702–19.
- Paguigan ND, et al. Enhanced dereplication of fungal cultures via use of mass defect filtering. *J Antibiot*. 2017;70:553–61.
- El-Elimat T, et al. High-Resolution MS, MS/MS, and UV database of fungal secondary metabolites as a dereplication protocol for bioactive natural products. *J Nat Prod*. 2013;76:1709–16.
- González-Medina M, et al. Scaffold diversity of fungal metabolites. *Front Pharm*. 2017;8:180.
- González-Medina M, et al. Chemoinformatic expedition of the chemical space of fungal products. *Future Med Chem*. 2016;8:1399–412.
- Mohammadipanah F, Matasyoh J, Hamed J, Klenk H-P, Laatsch H. Persipeptides A and B, two cyclic peptides from *Streptomyces* sp. UTMC 1154. *Bioorg Med Chem*. 2012;20:335–9.
- Ayers S, et al. Peptaibols from two unidentified fungi of the order *Hypocreales* with cytotoxic, antibiotic, and anthelmintic activities. *J Pept Sci*. 2012;18:500–10.
- Lichorowicz CL, et al. Synthesis of mono- and bisperoxide-bridged artemisinin dimers to elucidate the contribution of dimerization to antimalarial activity. *ACS Infect Dis*. 2021;7:2013–24.
- Panthama N, Kanokmedhakul S, Kanokmedhakul K, Soyong K. Cytotoxic and antimalarial azaphilones from *Chaetomium longirostre*. *J Nat Prod*. 2011;74:2395–9.
- Khumkomkhet P, Kanokmedhakul S, Kanokmedhakul K, Hahn-vajanawong C, Soyong K. Antimalarial and cytotoxic depsidones from the fungus *Chaetomium brasiliense*. *J Nat Prod*. 2009;72:1487–91.
- Waterman C, et al. Miniaturized cultivation of microbiota for antimalarial drug discovery. *Med Res Rev*. 2016;36:144–68.
- Calcul L, et al. Screening mangrove endophytic fungi for antimalarial natural products. *Mar Drugs*. 2013;11:5036–50.
- Harrison C. Patenting natural products just got harder. *Nat Biotechnol*. 2014;32:403–4.
- Gardes M, Bruns TD. ITS primers with enhanced specificity for basidiomycetes-application to the identification of mycorrhizae and rusts. *Mol Ecol*. 1993;2:113–8.
- PCR Protocols. A guide to methods and applications. Academic, 1990.
- Raja HA, Miller AN, Pearce CJ, Oberlies NH. Fungal identification using molecular tools: a primer for the natural products research community. *J Nat Prod*. 2017;80:756–70.
- Schoch CL, et al. Finding needles in haystacks: linking scientific names, reference specimens and molecular data for fungi. *Database (Oxf)*. 2014;2014:bau061.
- Wijayawardene N, et al. Outline of Fungi and fungus-like taxa. *Mycosphere*. 2020;11:1060–456.
- Hernández-Restrepo M, et al. The genera of fungi—G6: *Arthrographis*, *Kramasamuha*, *Melnikomyces*, *Thysanoreia*, and *Verrucosis*. *Fungal Syst Evol*. 2020;6:1–24.
- Zhang D, et al. PhyloSuite: an integrated and scalable desktop platform for streamlined molecular sequence data management and evolutionary phylogenetics studies. *Mol Ecol Resour*. 2020;20:348–55.
- Kalyanamoorthy S, Minh BQ, Wong TK, Von Haeseler A, Jermini LS. ModelFinder: fast model selection for accurate phylogenetic estimates. *Nat Methods*. 2017;14:587–9.
- Nguyen L-T, Schmidt HA, Von Haeseler A, Minh BQ. IQ-TREE: a fast and effective stochastic algorithm for estimating

- maximum-likelihood phylogenies. *Mol Biol Evol.* 2015;32:268–74.
40. Raja HA, Oberlies NH, Stadler M. Occasional comment: fungal identification to species-level can be challenging. *Phytochemistry.* 2021;190:112855.
41. Oduola AM, Weatherly NF, Bowdre JH, Desjardins RE. *Plasmodium falciparum*: cloning by single-erythrocyte micromanipulation and heterogeneity in vitro. *Exp Parasitol.* 1988;66:86–95.
42. Canfield CJ, Pudney M, Gutteridge WE. Interactions of atovaquone with other antimalarial drugs against *Plasmodium falciparum* in vitro. *Exp Parasitol.* 1995;80:373–81.
43. Trager W, Jensen JB. Human malaria parasites in continuous culture. *Science.* 1976;193:673–5.